Article

Anaerobic Fluidized-Bed Membrane Bioreactor for Treatment of Liquid Fraction of Sludge Digestate: Performance and Agricultural Reuse Analysis

Lu Liu [1], Jun Zhang [1,*], Yifan Chen [1], Ze Guo [1], Ganzhan Xu [1], Linlin Yin [1], Yu Tian [1] and Stevo Lavrnić [2]

[1] National Engineering Research Center For Safe Disposal and Resources Recovery of Sludge, School of Environment, Harbin Institute of Technology, Harbin 150090, China
[2] Department of Agricultural and Food Sciences, Alma Mater Studiorum-University of Bologna, Viale Giuseppe Fanin 40-50, 40127 Bologna, Italy
* Correspondence: hitsunyboy@126.com; Tel./Fax: +86-451-8628-3077

Abstract: The treatment of sludge digestion liquid is a big challenge in wastewater treatment. If treated as normal wastewater, large amounts of nitrogen and phosphorus present in the sludge digestion liquid might be wasted when they could be reused in agricultural irrigation and reduce the consumption of artificial fertilizers. Thus, it is of utmost importance to deliver a simple and feasible strategy to treat sludge digestion liquid for agricultural reuse. In this study, a novel type of anaerobic fluidized bed membrane bioreactor system (US-AnFMBR) was developed by combining an ultrasonic processing unit and biochar in AnFMBR. The improvement of sludge properties, removal of pollutants performance and membrane fouling mitigation were achieved in this novel system. The optimal dose of BC (biochar) was 2.5 g·L^{-1}, and the optimal ultrasonic treatment conditions were 30 min at 26 W. The main contribution of ultrasound was to improve the activity of sludge microorganisms to adsorb and degrade more organic matter present in sewage. The system achieved the removal efficiencies of COD, NH_4^+-N and PO_4^{3-}-P up to 89.41%, 49.29% and 54.83%, respectively, and had a better mitigation effect in terms of membrane fouling. On the one hand, the biochar addition for COD removal performance was mainly manifested in membrane rejection performance. On the other hand, the combination of low-cost biochar and AnFMBR can also provide new ideas for the recycling of agricultural waste for biochar production. However, regarding the removal efficiency of NH_4^+-N and PO_4^{3-}-P, the US-AnFMBR system promoted the activity of starved sludge to preferentially absorb NH_4^+-N compared with PO_4^{3-}-P by statistical analysis. The US-AnFMBR can reduce the viscosity of sludge and release more small molecular substances, thus better mitigating membrane fouling. Long-term operation performance also revealed the excellent stability of the sludge digestion liquid treatment. The US-AnFMBR system achieves the recovery of nitrogen and phosphorus resources for subsequent agricultural recycling, and avoids the eutrophication of water ecosystems. Reclaimed water meets the nutrient requirements of typical crops during the growing season. To a certain extent, carbon emission reductions in agriculture can be achieved.

Keywords: agricultural reuse; anaerobic fluidized-bed membrane bioreactor; ultrasonic; biochar; sludge digestion liquid; membrane fouling

1. Introduction

In the course of sewage treatment, the remaining sludge contains a large amount of toxic and harmful substances such as organic contaminants, pathogens and heavy metals [1–3] that, if improperly handled, can easily lead to secondary pollution of the environment [4]. Many technologies have been developed for the treatment and disposal of surplus sludge, such as landfill, compost, drying-incineration, anaerobic digestion, land application and recycling as building materials. Amongst them, anaerobic digestion is widely used in the sludge stabilization of urban sewage treatment plants because of

its ability to recover energy effectively and reduce pollutant discharge. In the process of anaerobic digestion of sludge, a large amount of organic matter is consumed and converted into methane [5,6]. At the same time, ammonia nitrogen cannot be converted in an anaerobic environment; instead, it can accumulate due to denitrification [7]. Due to the anaerobic release of phosphorus, its concentration in the liquid phase of sludge can be rather high. For example, the ammonia nitrogen concentration (NH_4^+-N) and COD in the sludge digestion liquid are in a range of 500–1500 $mg \cdot L^{-1}$ and 500–1000 $mg \cdot L^{-1}$, respectively, casing a carbon/nitrogen ratio less than 1, and phosphate (PO_4^{3-}-P) can also be as high as 200 $mg \cdot L^{-1}$. Therefore, there is a large amount of nitrogen and phosphorus in the sludge digestion liquid [8]. In China, the digested sludge is rarely treated separately, and it is usually returned to the biological treatment unit together with raw water. Its water volume only accounts for about 2% of the sewage treatment plant, but it contains 15–25% ammonia nitrogen and 20–80% phosphate, which greatly increases the operating load of the sewage treatment plant and does not conform to the current concept of recycling the resources in the sewage [9,10].

The main difference in the treatment process of sludge digestion liquid is the removal of ammonia nitrogen. At present, the treatment process and technology of sludge digestion liquid mainly include conventional nitrification and denitrification, short-cut nitrification-denitrification, anaerobic ammonia oxidation, magnesium ammonium phosphate and so on, but these processes have their own shortages. Conventional nitrification and denitrification processes consume a large number of organics, and their application in the treatment of sludge digestion often requires an external carbon source. Wang et al. [11] successfully achieved simultaneous nitrification and denitrification by using SHBR reactors to limit the airflow to prevent the formation of nitrates, with a total nitrogen removal rate increased from 68% to 85%, but it required a sophisticated reactor and strictly controlled operating conditions. In addition, during the reaction process, N_2O and other greenhouse gases were causing or resulting. Short-cut nitrification-denitrification denitrification process has the problem of difficult control of operating parameters. Claros et al. [12] used sensors to precisely adjust the amount of nitrite and enhance the removal of ammonia nitrogen. It greatly reduced the ammonia nitrogen concentration of the effluent and increased the ammonia nitrogen removal rate to 98%, but there were still many problems in practical applications, such as how to control the DO and pH in the reactor accurately, and how to operate the reactor in a stable way at room or even low temperature. The anammox process has problems such as a slow growth rate and a long start-up period, which is difficult to apply in practice [13,14]. The resource recovery process represented by magnesium ammonium phosphate often has the problem of higher cost due to a large amount of processing [15,16]. Therefore, many researchers have proposed to treat the sludge digestion liquid separately.

Membrane water treatment and reuse is a cutting-edge technology to curb the deterioration of the ecological environment, reduce system energy consumption, achieve water quality improvement, and resource and energy recovery. Anaerobic membrane bioreactor (AnMBR), as one of the most representative water treatment technology, receives extensive attention due to its low energy consumption, high organic load, low sludge production, recyclable biogas energy and impact load resistance [17], and is widely used in food processing wastewater, industrial wastewater, wastewater containing high-concentration solids and municipal wastewater treatment [18]. Compared with the aerobic process, AnFMBR does not require aeration, which greatly reduces the energy consumption of the reactor [19]. Seib et al. [20] found that compared with aerobic membrane bioreactor (0.3–0.6 kWh m^{-3}), anaerobic membrane bioreactor (0.05–0.13 kWh m^{-3}) can greatly reduce energy consumption. Gao et al. [21] studied the treatment of domestic sewage by AnFMBR and found that the removal rates of COD were 74.0 ± 3.7%, 67.1 ± 2.9% and 51.1 ± 2.6% at 35 °C, 25 °C and 15 °C and that granular activated carbon (GAC) can reduce membrane fouling by absorbing protein, the main pollutant. Xiao et al. [22] reduced membrane fouling by forming cross-flow conditions in the AnMBR system and found that the COD removal rate can reach 99% when studying the efficiency of the system for treating kitchen wastewater. Ying et al. [23] reported that excessive

dosing of powder-activated carbon (PAC) might block the membrane pores and accelerate the formation of the mud cake layer for its small particle size deposition on the surface of the membrane, which will bring negative effects to a certain extent. Chaiprapat et al. [24] found that under the minimum liquid/gas ratio (0.6 V/V) to maintain GAC fluidization conditions, the membrane fouling rate was reduced by 90% compared with the pure gas injection (no activated carbon medium flushing) technology.

Biochar is a porous, carbon-rich product produced by the pyrolysis of biomass under oxygen-limited conditions [25]. Biochar has many good properties as an environmentally friendly and cost-effective material for carbon sequestration, energy recovery and soil improvement [26]. Biochar is widely used as an effective adsorbent for water pollution treatment. The application of biochar in bioreactors is currently in an emerging state. Pretreatment of the feed wastewater by adding biochar to an anaerobic membrane bioreactor pretreatment of the feed wastewater can effectively mitigate membrane fouling by changing the feed characteristics [27]. In addition, biochar exists to facilitate the release and recovery of nitrogen and phosphorus from thickened sludge. With the addition of biochar to the bioreactor, the thickened sludge releases more PO_4^{3-}-P and NH_4^+-N, obtaining a continuous supply of nitrogen and phosphorus. This is a promising method for recycling nitrogen and phosphorus from thickened sludge [28].

Ultrasound not only has the effect of elution, but it also can strengthen the activity of sludge at a certain intensity, so using ultrasound to treat the saturated sludge can restore its adsorption capacity. Maria et al. [29] studied the effect of ultrasonic treatment on the dewatering effect of secondary sludge and found that the total solid content of ultrasonic treatment sludge increased by 16.2% after centrifugation, and the dewatered sludges had lower levels of viscosity and thixotropy than untreated sludge. Zhang et al. [30] found that the sludge treatment volume increased by 28%, and the biomass growth rate increased by 12.5% under the treatment conditions of 25 kHz (sound frequency), 0.2 W mL^{-1} (power density) and 30 s (ultrasonic time). However, the pure anaerobic process does not have a removal effect on nitrogen and phosphorus, but it has strong adsorption capacity. In previous studies, it was seen that ultrasonically coupled anaerobic bioreactors have great potential for engineering applications, not only to increase the activity of anaerobic organisms but also to increase the production of CH_4 [31,32]. Ultrasound causes the sludge to release nitrogen, phosphorus and COD [33,34]. The supernatant of the sludge after ultrasound treatment contains high levels of nitrogen and phosphorus, which is very beneficial for the recovery of these nutrients. However, excessive organic carbon sources will affect the recycling of nitrogen and phosphorus and cause the system to collapse in severe cases [35]. The sludge needs to be allowed to release the adsorbed nitrogen and phosphorus without the remaining sludge flocs being destroyed. Therefore, reasonable control of the intensity of ultrasound is required for the recovery of nitrogen and phosphorus from residual sludge in anaerobic digestate treatment.

Herein, we present a new strategy to treat sludge digestion liquid. In the present work, the biochar was synthesized successfully, and the synergistic effect of ultrasonic treatment and biochar was explored by evaluating the removal of COD, NH_4^+-N and PO_4^{3-}-P and mitigation of membrane fouling in the AnFMBR system under long-term operation. Moreover, the mechanism of membrane fouling mitigation was explored by TMP (transmembrane pressure), FT-IR (Fourier Transform infrared spectroscopy) and EEM (excitation-emission matrix). Finally, the agricultural and environmental benefits of the reactor effluent were analyzed using the agricultural conditions in a Chinese context. It was explored whether the experimental effluent had the N and P concentrations required to meet the crop growth demands. Further, the greenhouse gas reduction benefits of using the reactor effluent as agricultural irrigation water were estimated.

2. Material and Methods

2.1. Preparation of Biochar

The biochar used in this experiment was prepared by pine sawdust in a tube furnace with N_2 as the carrier gas and treated at 500 °C for 0.5 h, followed by cooling to room temperature before collection. The prepared biochar was grounded and sieved to make the particle size between 40–200 mesh (0.075–0.42 mm).

2.2. Setup of the AnFMBR System

The laboratory scale AnFMBR system was used to run the whole experiment, as shown in Figure 1. The system consisted of a wastewater supply tank, a wastewater supply pump, an anaerobic fluidized bed membrane bioreactor (main reactor), a membrane module, an ultrasonic unit, a circulating pump, a TMP meter, a storage water pump and a storage water tank. The main reactor, with an effective volume of about 9 L, was coated with a heating cover to maintain the working temperature at the mesophilic range of 35 ± 1 °C. There were three circulating water inlet holes at the bottom of the reactor to increase the fluidization efficiency, reduce the static zone at the bottom of the reactor, and flush the membrane surface to reduce membrane pollution. A three-phase separator was installed at the top of the reactor to prevent sludge from entering the water recirculation process.
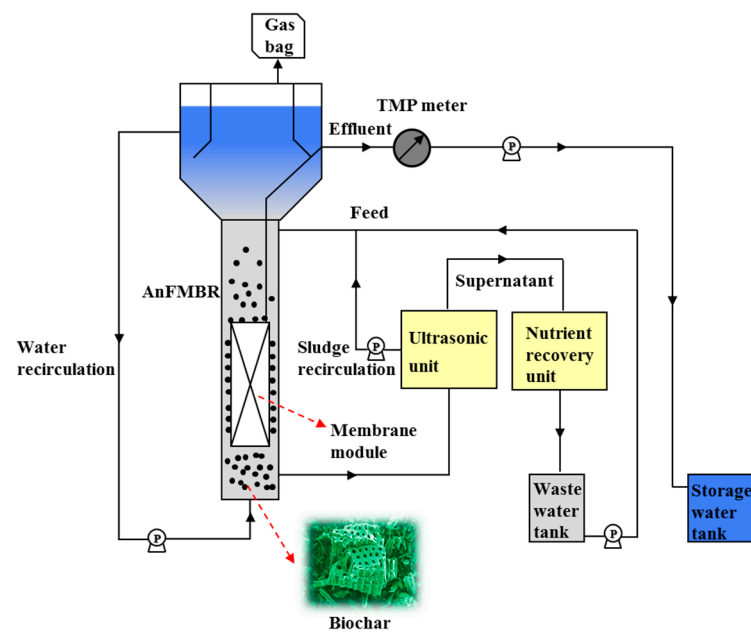

Figure 1. Schematic diagram of US-AnFMBR system.

The wastewater supply tank was filled with synthetic wastewater, with a composition listed in Table 1, that continuously entered the AnFMBR reactor through a peristaltic pump. The seed sludge was collected from Taiping Sewage Treatment Plant anaerobic tank in Harbin, China, and acclimated before commencing the experiment with a mixed liquid suspended solid (MLSS 5000 mg·L^{-1}). The returned sludge entered the ultrasonic unit through the bottom of the reactor. After ultrasonic treatment, the supernatant flows into a nutrient (nitrogen and phosphorus) recovery unit. In the nutrient recovery unit, a blow-off test is carried out to recover nitrogen and a magnesium phosphate precipitation test to recover phosphorus, which then flows into the wastewater supply tank, while the settled sludge is returned to the reactor. The process was carried out intermittently. The membrane module was immersed in the cylindrical side stream reactor with hollow fiber membrane with a surface area of 59.5 cm^2, adopted from Tianjin Motian Membrane Technology Co., Ltd, (Tianjin, China). The treated water was collected in a storage water

tank through a storage water pump. The gas generated during the operation of the reactor was collected in a gas bag.

Table 1. Composition of the synthetic influent wastewater.

Component	Concentration (mg·L^{-1})	Component	Concentration (mg·L^{-1})
Starch	100	$ZnSO_4$	0.43
NH_4Cl	2000	$MnCl_2 \cdot 4H_2O$	0.99
KH_2PO_4	44	$CuSO_4 \cdot 5H_2O$	0.25
K_2HPO_4	56	$NiCl_2 \cdot H_2O$	0.19
$MgSO_4 \cdot 7H_2O$	54	H_3BO_4	0.014
$CaCl_2 \cdot 2H_2O$	147	$NaMoO_4 \cdot 2H_2O$	0.22
$NaHCO_3$	1000	$CoCl_2 \cdot 6H_2O$	0.24

2.3. The Effects of Ultrasound and Biochar on the Sludge

The release of COD, NH_4^+-N and PO_4^{3-}-P was tested on 50 mL of anaerobic sludge samples with MLSS of 5000 mg·L^{-1}. The effect of ultrasound on sludge release was studied at 5, 10, 15, 20, 30, 40, 50 and 60 min and at 6.5, 13, 19.5, 26, 32.5, 39, 45.5 and 52 W at a pulse ratio of 3:1, respectively. This was followed by experimental studies on the release of COD, NH_4^+-N and PO_4^{3-}-P from sludge at 0, 2.5, 5 and 10 g·L^{-1} biochar dosages under optimal ultrasound conditions, respectively.

2.4. Long-Term Operation Performance of the AnFMBR System

In order to further study the long-term operating performance of the AnFMBR system, two AnFMBR reactors were tested under the same operating conditions. One reactor had a biochar addition (US-AnFMBR), and another one was without biochar (C-AnFMBR). First, both reactors were performed without ultrasonic treatment of sludge at the first 30 days (S1 and S3 for C-AnFMBR and US-AnFMBR, respectively) and with ultrasonic treatment of sludge at the next 30 days (S2 and S4 for C-AnFMBR and US-AnFMBR, respectively). The hydraulic retention time (HRT) was 36 h, the ultrasonic reflux time was 24 h and the fluidized bed rising flow rate was 5 cm·min^{-1}, respectively.

2.5. Water Sample Analyzes

The concentrations of COD, NH_4^+-N and PO_4^{3-}-P of the water during the operation phase of the reactor were analyzed by standard methods to evaluate the system treatment efficiency for sludge digestion liquid. The solution pH was measured by using the pH meter (PHSJ-3F, Lei Ci Instrument Factory, Shanghai, China). Soluble microbial products (SMP) and extracellular polymeric substances (EPS) as microbial metabolism products were major by-products that contribute to membrane fouling through cake formation [36–38]. Their main components are proteins and polysaccharides. To extract SMP, bulk liquid collected in the reactor was centrifuged (5000 rpm, 5 min). The supernatant was filtered using a 0.45 μm syringe filter. EPS extraction was performed using the thermal treatment method [39]. The above mud sample was brought to a constant volume (59 mL) with distilled water, then heated at 80 °C in a water bath for 30 min. Subsequently, the solution was centrifuged under the same conditions to obtain the supernatant containing SMP and EPS. In this experiment, the total amount of protein and polysaccharide was used as the quantitative standard of SMP and EPS. The concentration of polysaccharide was determined by phenol–sulfuric acid method [40], and the standard curve was drawn with a standard glucose solution. The protein concentration was determined by using a high/low concentration Lowry kit method [41], and the standard curve was plotted by using a bovine serum protein standard solution.

The morphology of the biochar was observed on a Quanta 200 scanning electron microscopy (SEM) with an operating voltage of 10.0 kV.

Three-dimensional excitation-emission matrix (3D-EEM) fluorescence spectra of the SMP were measured by a fluorescence spectrometer (Jasco FP-6500), and ultrapure water

was taken as a blank. Excitation and emission slits were maintained at 5 nm, and the scanning speed was set at 1200 nm·min^{-1}. The excitation light wavelength and the emission light wavelength both range from 220~650 nm, and the scanning step length was 2 nm. After scanning, the instrument would automatically calibrate the fluorescence spectrum.

2.6. Data Statistical Analyzes

The Pearson correlation coefficient measures a linear dependence between two variables, and it is the most commonly used method in the correlation test. Following the standardization of data, the Pearson correlation coefficient is calculated by Formula (1):

$$r = \rho_{X,Y} = \frac{cov(X,Y)}{\sigma_X \sigma_Y} = \frac{E[(X - \mu x)(Y - \mu y)]}{\sigma_X \sigma_Y} = \frac{\sum(x - E(X))(y - E(Y))}{\sqrt{\sum(x - E(X))^2 \sum(y - E(Y))^2}} \tag{1}$$

$cov(X, Y)$ is the covariance, which can be calculated by Formula (2):

$$\begin{aligned} Cov(X, Y) &= E[(X - E[X])(Y - E[Y])] \\ &= E[XY] - 2E[X]E[Y] + E[X]E[Y] \\ &= E[XY] - E[X]E[Y] \end{aligned} \tag{2}$$

$E[X]$ (or $E[Y]$) is the mean value.

The corresponding linear correlation matrix can be obtained by calculating the Pearson correlation coefficient between each indicator.

3. Result and Discussion

3.1. Morphology and Hydrophobicity of the Biochar

The morphology of biochar was observed by SEM. It can be seen from Figure 2a that the biochar prepared by pine sawdust presented an irregular multi-layer structure with many irregular pores and channels on the material and some wrinkles on the surface, which greatly increased the specific surface area. It not only served as a good adsorbent, but its irregular surface also provided a good place for the growth of microorganisms. In addition, the hydrophilic and hydrophobicity of the biochar was tested. As shown in Figure 2b, the contact angle of biochar was 120°, greater than 90°, indicating that it has a high hydrophobicity [42].
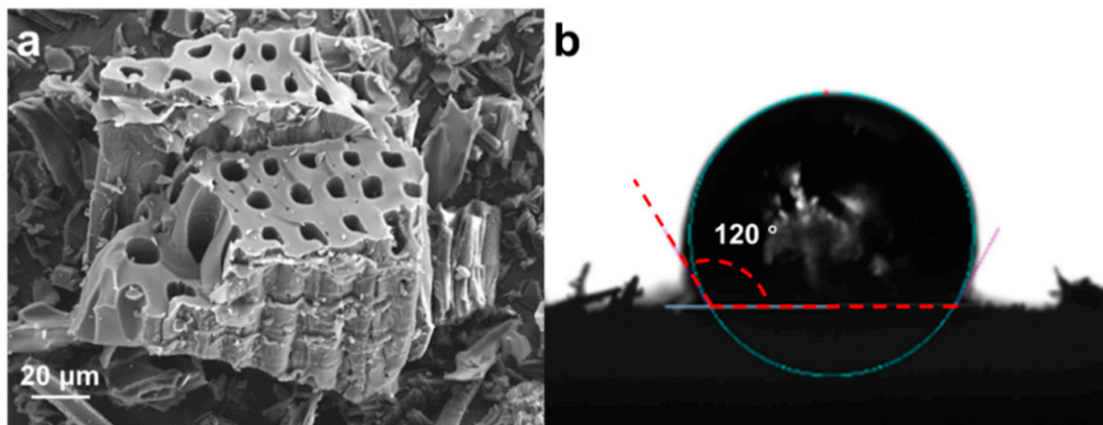

Figure 2. (**a**) SEM and (**b**) contact angle images of the biochar.

3.2. Ultrasonic and Biochar Effect on Sludge Solubilization

3.2.1. Ultrasonic Effect on Sludge Solubilization

The solubilization process of sludge pollutants with time under the ultrasonic power condition of 13 W is shown in Figure 3a. It can be seen that as the ultrasound time progresses, the concentrations of NH_4^+-N, PO_4^{3-}-P and COD increased from 565.43 mg·L^{-1}

to 708.29 mg·L^{-1}, 71.02 mg·L^{-1} to 133.28 mg·L^{-1}, and 666.40 mg·L^{-1} to 4050.66 mg·L^{-1}, respectively. Compared with the solubilization of COD, that of NH_4^+-N and PO_4^{3-}-P were relatively slow, especially within 40 min. The amount of COD and protein did not increase during the 20–40 min, but there was a drastic increase after 40 min, which indicated that the flocs were broken and the cell walls of bacteria were disrupted, leading to the releases of organic compounds. Therefore, the recommended ultrasound time was 30 min.
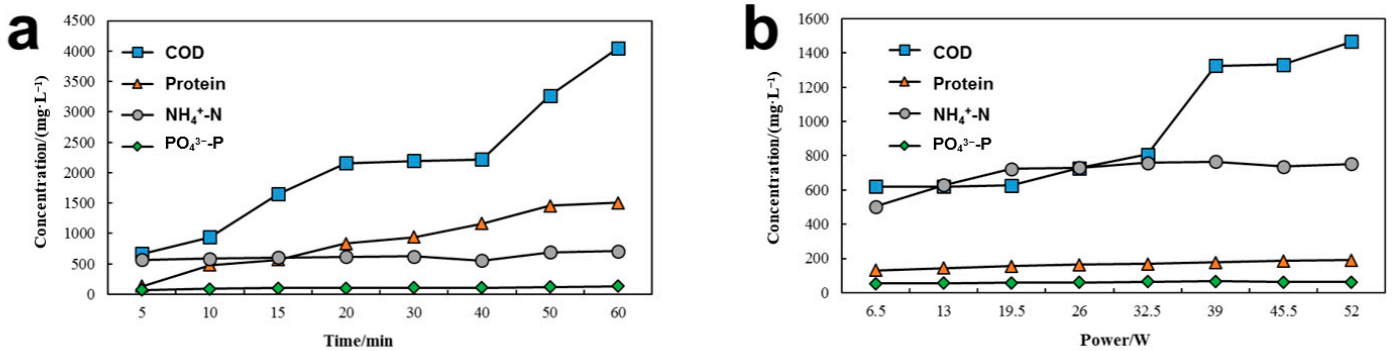

Figure 3. Solubilization process of sludge pollutants depending on (**a**) Time and (**b**) Power.

The effect of ultrasonic power on the solubilization process of sludge pollutants under the ultrasonic time of 30 min is shown in Figure 3b, and it can be seen that with the power increasing, the concentrations of NH_4^+-N and PO_4^{3-}-P also increased. The concentration of NH_4^+-N increased from 502.53 mg·L^{-1} to 751.38 mg·L^{-1}, but the solubilization was particularly limited when the power exceeded 19.5 W. The concentration of PO_4^{3-}-P increased from 54.55 mg·L^{-1} to 63.73 mg·L^{-1}, relatively lower than that of COD and NH_4^+-N, indicating that the ultrasonic power had little effect on the solubilization of PO_4^{3-}-P. The COD concentration increased from 619.36 mg·L^{-1} to 1466.08 mg·L^{-1}. It can be found that the effect of ultrasonic power on sludge was not as great as the ultrasonic time, but the COD had a greater increase after the power exceeded 32.5 W, indicating that the higher mechanical shear forces produced at higher powers ruptured the cell walls of microorganisms and thereby increased the COD [43]. Therefore, the recommended power was 26 W. The optimum sonication conditions for the release of nutrients from the residual sludge without destroying the residual sludge floc are 26 W for 30 min. This confirms the significant potential for nutrient recovery and reuse of the sludge produced by the ultrasonic treatment of AnFMBR when treating anaerobic digestate.

3.2.2. Biochar Effect on Sludge Solubilization

The effect of different biochar concentrations on sludge was studied under certain ultrasonic treatment conditions (30 min, 26 W). As shown in Figure 4a–c, the influences of biochar concentration on COD, NH_4^+-N and PO_4^{3-}-P solubilization were tested. It can be seen from Figure 4a,b that the COD and NH_4^+-N in the sludge had the best solubilization effect when the biochar concentration was 5 g·L^{-1}. When the concentration increased to 10 g·L^{-1}, the solubilization effect was reduced, which indicated that the proper concentration of biochar could cause the release of COD and NH_4^+-N during the ultrasonic treatment, but the addition of excessive biochar would prevent the release of COD. As shown in Figure 4c, the best biochar concentration for PO_4^{3-}-P release was 2.5 g·L^{-1}. Similarly, with the increase of the biochar concentration, the solubilization effect decreased, even lower than in a solution without biochar. It may be due to the dissolved phosphate being adsorbed by the biochar since the biochar had a strong binding energy to the phosphate.
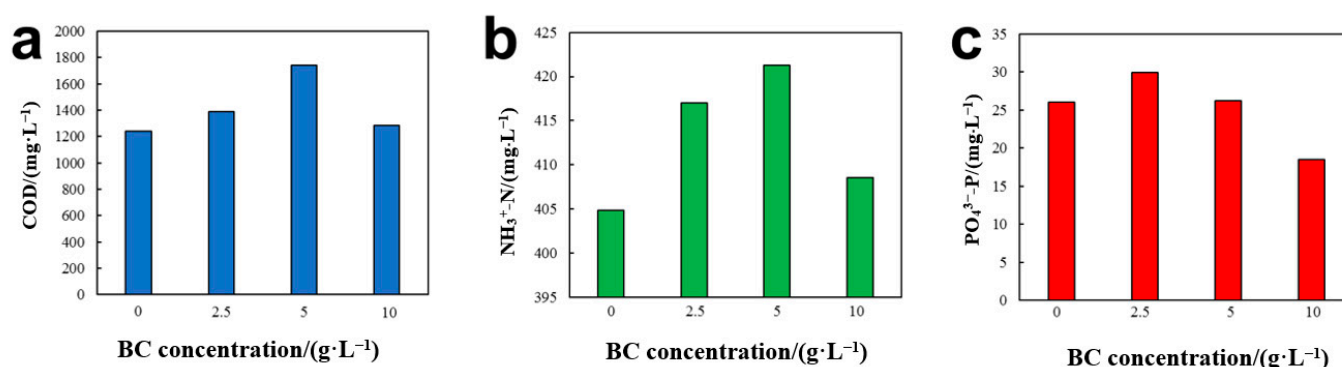
Figure 4. Solubilization effect of sludge pollutants with different biochar concentrations (**a**) COD, (**b**) NH_4^+-N and (**c**) PO_4^{3-}-P.

Furthermore, the viscosity of the sludge was studied. It can be seen from Table 2 that the viscosity of the sludge was reduced from 3.02 mPa·s to 2.46, 2.28 and 2.80 mPa·s as biochar concentration increased. The addition of biochar was beneficial to reducing the sludge viscosity to a certain degree since there was a large number of EPS on the surface of the sludge, which were easily attracted to each other and therefore enhanced the sludge viscosity. The proper concentration of biochar can reduce the probability of collision among sludge particles, thereby reducing the viscosity of the sludge and promoting the solubilization process of sludge pollutants. However, excessive biochar would cause the viscosity increase and hinder the solubilization of pollutants, which was unfavorable for the treatment of sewage. There is a positive effect of ultrasound and biochar on the release of nutrients from sludge dissolution, providing a basis for subsequent nutrient recovery (see Figures S1 and S2).

Table 2. Sludge viscosity at different biochar concentrations.

Biochar Concentration (g·L^{-1})	0	2.5	5	10
Viscosity (mPa·s)	3.02	2.46	2.28	2.80

3.3. Long-Term Operation Performance

3.3.1. Pollutants Removal Performance in Two Systems

The long-term operating performance of the two AnFMBR systems for pollutant removal was studied. COD is an important indicator for judging water quality, and its concentration in two systems is shown in Figure 5a. The average COD removal rates at S1, S2, S3 and S4 were 68.15%, 87.58%, 71.67% and 89.41%, respectively (Figure 5b), which indicated that the sludge played a positive effect on COD removal from S1. Comparing with the removal rate of COD at S1, that at S3 improved slightly indicating that the biochar had a positive effect on COD removal because of its adsorption. In addition, under the action of ultrasonic treatment of sludge, the removal rate of COD had increased by nearly 20% at S2 and S4. Moreover, S4 had the highest COD removal rate, which indicated that the coupling system had an effective COD removal effect.

The NH_4^+-N and PO_4^{3-}-P removal performance were also analyzed for each of the two systems. As the concentration of NH_4^+-N and PO_4^{3-}-P shown in Figure 6a,b indicate, there were no removal effects at S1 and S3. Considering the limited adsorption capacity of biochar, the addition of biochar had little effect on NH_4^+-N and PO_4^{3-}-P. However, the removal rate of both NH_4^+-N and PO_4^{3-}-P had an obvious increase at S2 and S4, as shown in Figure 6c. The average removal rates of NH_4^+-N at S2 and S4 were 43.52% and 49.29%, respectively, and the average removal rates of PO_4^{3-}-P at S2 and S4 were 49.05% and 54.83%, respectively. Generally, the utilization of NH_4^+-N by microorganisms tended to be stable in an anaerobic environment, especially when the system did not involve the discharge of extra sludge. In addition, the sludge flocs precipitated at the bottom of the

reactor and began to hydrolyze, converting intracellular organic nitrogen into NH_4^+-N and finally increasing the effluent concentration of NH_4^+-N (Figure 6a). However, the lower NH_4^+-N concentration at S2 and S4 emphasized the function of low-density ultrasound to achieve the removal of NH_4^+-N, which was similar to the mechanism of absorption of NH_4^+-N by sludge. Similarly, the endogenous respiration of sludge in a state of starvation after ultrasonication promoted the further release of PO_4^{3-}-P. Once the sludge was deficient in PO_4^{3-}-P, the microorganisms would slowly absorb the PO_4^{3-}-P from wastewater.
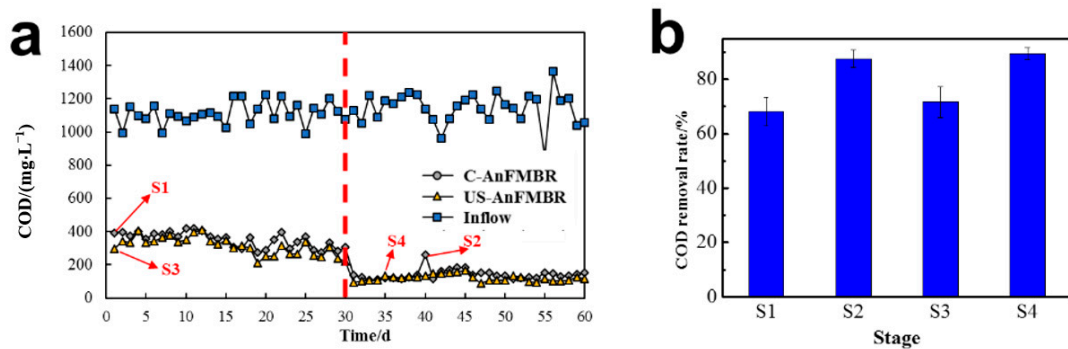

Figure 5. (**a**) COD variation with time in two systems and (**b**) COD removal rate at different stages (S1:C-AnFMBR, at first 30 days; S2:C-AnFMBR, at next 30 days; S3:US-AnFMBR, at first 30 days; S4:US-AnFMBR, at next 30 days).
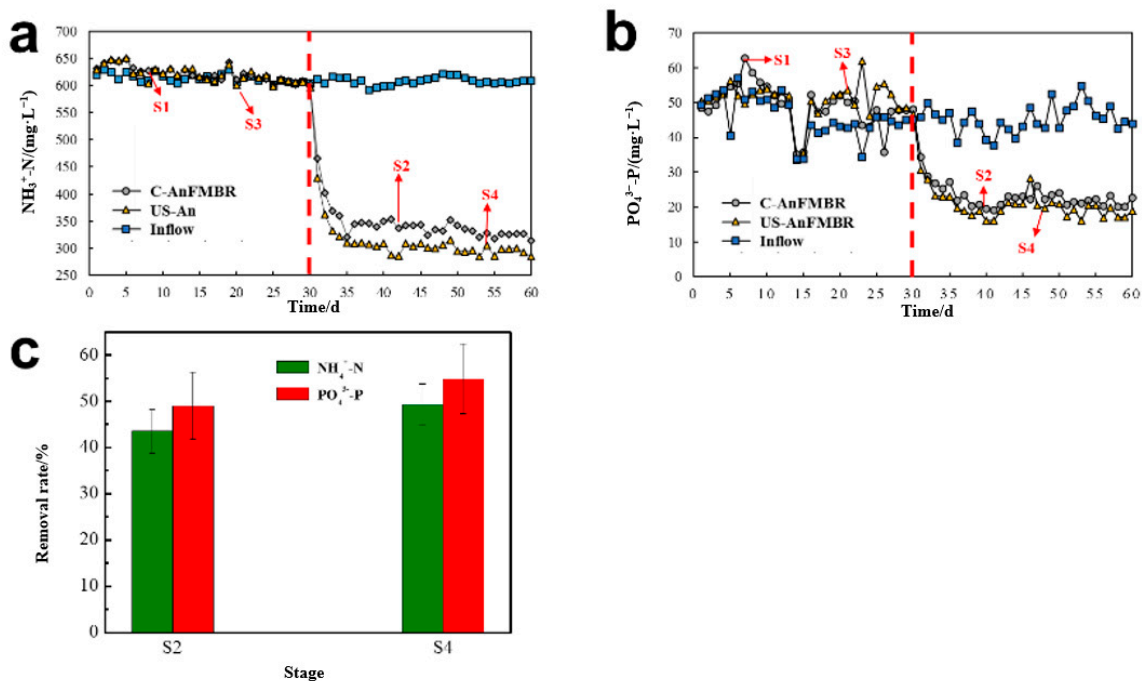

Figure 6. (**a**) NH_4^+-N and (**b**) PO_4^{3-}-P variation with time in two systems and (**c**) the removal rate at different stages.

As mentioned above, pollutant removal efficiencies were improved due to the simultaneous introduction of ultrasound and biochar based on control AnFMBR. In order to further explore the wastewater treatment behavior in US-AnFMBR, the Pearson correlation coefficient was used to analyze the statistical correlation between a series of condition parameters (including ultrasound and biochar) and pollutants removal efficiencies. The results showed that the ultrasound was significantly associated with COD removal ($\rho = 0.735$, $p = 0.001$), NH_4^+-N removal ($\rho = 0.457$, $p < 0.001$) and PO_4^{3-}-P removal ($\rho = 0.120$, $p = 0.001$). Especially, the ultrasound exhibited prominent removal efficiencies of COD and NH_4^+-N

($\rho COD > \rho NH_4^+$-N $> \rho PO_4^{3-}$-P). Additionally, the statistical analysis of the correlation between biochar and pollutants removal showed that the concentration of biochar was also related to the removal of pollutants ($\rho COD = 0.682$, ρNH_4^+-N $= 0.103$, ρPO_4^{3-}-P $= 0.099$). Above all, it illustrated that the synergistic effect of ultrasonic and biochar in the US-AnFMBR system promoted the activity of starved sludge to preferentially absorb NH_4^+-N compared with PO_4^{3-}-P.

3.3.2. Membrane Filtration Performance in Two Systems

Stability in flux or transmembrane pressure (TMP) is the most critical parameter for the applicability and economic feasibility of AnFMBRs treating sludge for long-term operation. The membrane fouling was observed by monitoring TMP. TMP refers to the difference in pressure from the feed side of the membrane to the permeate side of the membrane [44,45], and a higher TMP implies more severe fouling [46,47]. Figure 7 shows the stepwise increase of TMP of US-AnFMBR and C-AnFMBR during the long-term operating performance. It can be observed that the increased rates of membrane fouling can be greatly reduced at S4. Therefore, compared with C-AnFMBR, the membrane permeability got obviously improved by the synergistic system of US-AnFMBR. It is well acknowledged that the liquid shear and mechanical scouring by the fluidized media mitigate membrane fouling in the AnFMBRs [48]. Compared with C-AnFMBR, the relatively lower TMP in US-AnFMBR indicated the significant antifouling effect of the fluidized biochar by inducing an unsteady-state shear force on the membrane surface. This was exactly reflected by the result that the TMP at S3 and S4 were accordingly lower than that at S1 and S2 (Figure 7). Moreover, the US-AnFMBR system had a longer time to achieve stable conditions with a lower TMP, indicating that the ultrasonic treatment of sludge with biochar prolonged the duration of the membrane. The increase of TMP may be relevant to the deposition of material within pores, and this accumulation would take some time [49,50]. The authors believe that it was the ultrasound that changed the sludge properties and therefore influenced the flow rate and shear rate after sludge recirculation, decreasing the fouling layer thickness and fouling density [51,52]. Consequently, the slow growth of the fouling layer slowed down the rate of flux decline.
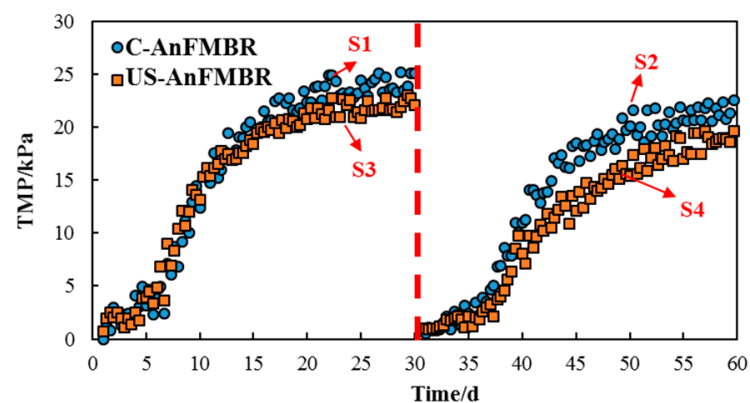

Figure 7. TMP of the dynamic membrane over the operation period.

3.4. Mechanisms of Pollutants Removal and Membrane Fouling Mitigation

3.4.1. Mechanisms of Pollutants Removal

In order to further analyze the removal performance of two systems, the membrane rejection rate of COD (COD_M) and microorganism removal rate of COD (COD_B) were calculated, respectively, and the results are shown in Figure 8. The average COD_M at S1, S2, S3 and S4 were 9.41%, 15.26%, 12.55% and 18.91%, respectively. Moreover, the average COD_B at S1, S2, S3 and S4 were 58.68%, 72.31%, 59.11% and 70.50%, respectively.
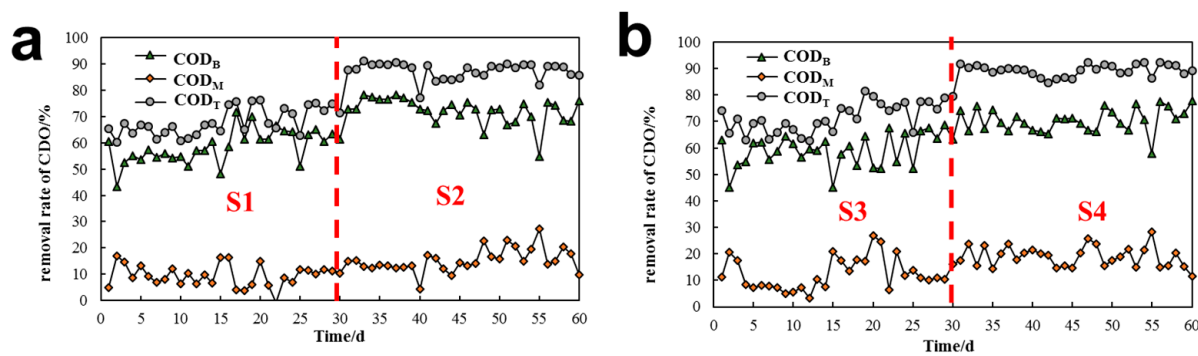
Figure 8. COD removal rate with time in (**a**) C-AnFMBR and (**b**) US-B-AnFMBR.

By comparing the COD removal rate of S1 and S2, it is found that the removal of COD_B was greatly improved from 58.68% to 72.31% after the ultrasonic treatment of sludge. The reason behind this may be the desorption of the organic matter that adsorbed on the sludge, causing the sludge in a state of starvation to degrade more organic matter after the ultrasonic treatment. Pilli et al. [53] found that sludge in a state of starvation could slightly enhance its microbial enzyme activity to absorb relatively more pollutants. The ultrasonic treatment can also enhance the removal rate of organic matter by changing the sludge's physicochemical properties and strengthening the sludge digestion [54,55]. By comparing the COD of S1 and S3, it was found that the COD_M removal slightly increased from 9.41% to 12.55%, which indicates that biochar had a certain positive effect on COD removal performance by improving the membrane rejection performance of COD. Meanwhile, the addition of biochar provided extra space for microbial adhesion and promoted the formation of granular sludge, which was advantageous to COD removal [56,57]. By comparing the COD of S1 and S4, both COD_M and COD_B increased from 9.41% to 18.91% and 58.68% to70.50%, respectively, which indicates that the COD removal performance was improved significantly by the synergistic effect of ultrasound and biochar. However, Joshi et al. [58] reported that a hydrogen peroxide and ultrasound pretreatment resulted in a COD solubilization of 40% when a dose of 50 g H_2O_2/kg TS and sonication for 60 min was employed. So, the synergistic effect of ultrasound and biochar has a promising effect on COD removal.

3.4.2. Mechanisms of Membrane Fouling Mitigation

According to the performance of the systems at different stages, the sludge and supernatant samples at S1, S2, S3 and S4 were selected for studying the mechanism of membrane fouling mitigation. The protein and polysaccharide contents of SMP and EPS are shown in Figure 9.
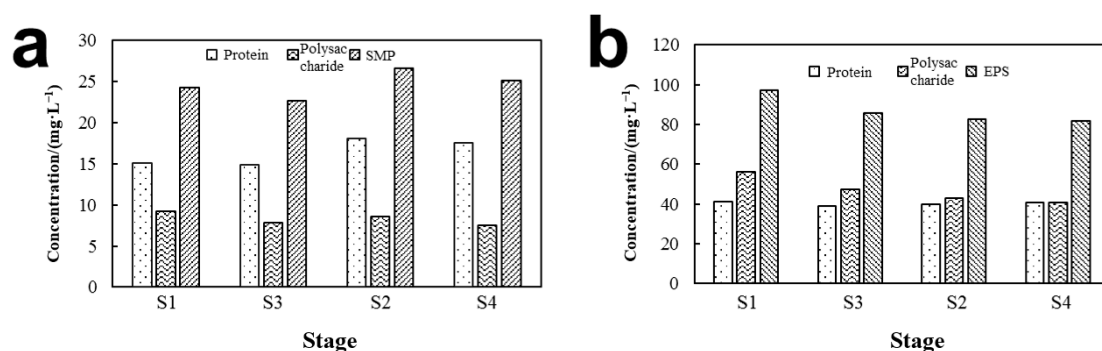

Figure 9. (**a**) SMP and (**b**) EPS concentration at different stages.

The average SMP concentrations of the two systems increased slightly from 24.33 mg·L^{-1} (S1) and 22.73 mg·L^{-1} (S3) to 26.65 mg·L^{-1} (S2) and 25.13 mg·L^{-1} (S4) after the ultrasonic

treatment (Figure 9a). Hence, adding biochar was beneficial to reduce the SMP in the system, while ultrasonic treatment, on the other hand, would increase the SMP. Generally speaking, a higher SMP concentration was more susceptible to affecting the membrane permeability of MBR and inducing membrane fouling [59]. In this study, however, C-AnFMBR with lower SMP concentration showed a higher membrane fouling rate than US-AnFMBR. Therefore, it was believed that changes in the properties of SMP may be one of the reasons for the reduction of membrane fouling in US-AnFMBR. In order to identify the fingerprints of this organic material, three-dimensional EEM spectra were applied to provide more information about the constituents of SMP, as shown in Figure 10. The fluorescence spectra generally gave three main peaks: peak A (Ex/Em 280/328 nm in S3,4 and 280/340 nm in S1,2), peak B (Ex/Em = 355/440 nm in all stages), and peak C (Ex/Em = 265/450 nm in all stages), being related to tryptophan protein-like substances, humic acid-like substances and aromatic protein or fulvic acid-like substances, respectively, although its intensity was quite weak in all the fluorescence spectra [60]. The fluorescence intensity (peak A in Figure 10) of US-AnFMBR was higher than that of C-AnFMBR, suggesting that the content of tryptophan protein-like substances in US-AnFMBR increased. This phenomenon may be associated with that of the ultrasonication treatment, and the addition of biochar enhanced the sludge activity to promote microorganisms to absorb more pollutants and decompose macromolecules into smaller ones. In addition, the intensities of peak B and peak C were very weak, illustrating that the concentration of humic acids and aromatic proteins or fulvic acids in these samples was very low. Humic acids and aromatic proteins or fulvic acids substances belonged to non-biodegradable organic matter, which had a small size and hence could easily pass through the membrane. According to the above analysis, the high SMP concentration in US-AnFMBR was mainly due to the increase of small molecular substances (such as the decomposition of tryptophan protein-like substances, humic acids, aromatic proteins or fulvic acids). Therefore, they may pass through the membrane more easily, resulting in a small impact on membrane scaling. In summary, these results suggested that the changes in characteristics of SMP after introducing ultrasonication and biochar into AnFMBR may be one of the reasons for the reduction of membrane contamination in US-AnFMBR.
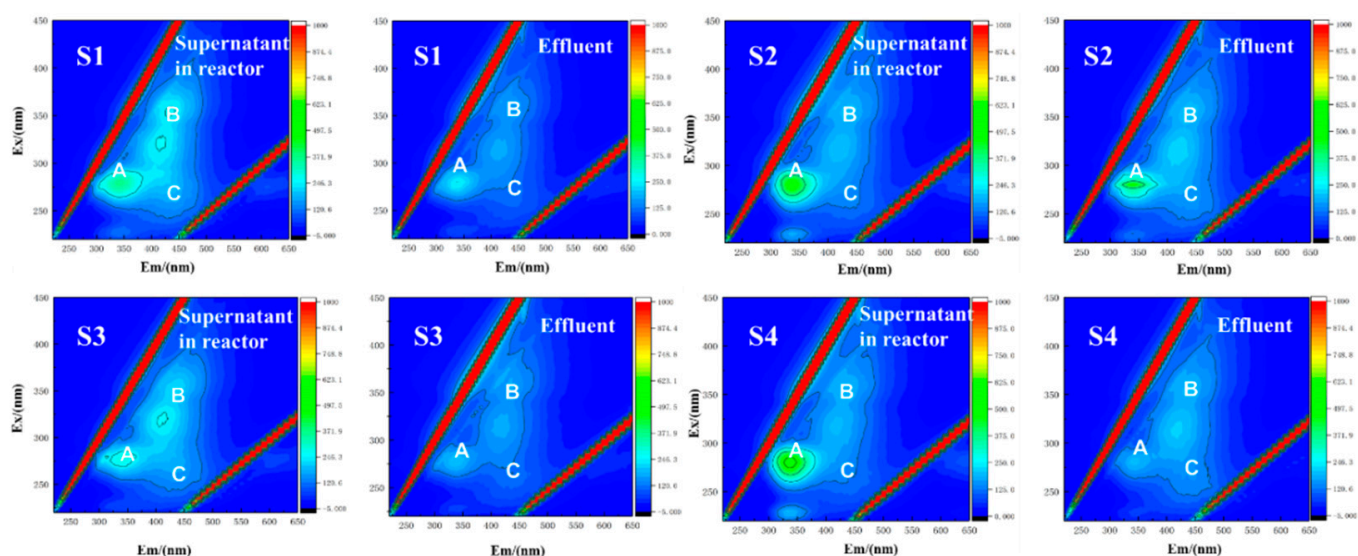

Figure 10. EEM fluorescence spectra of supernatant in reactor and effluent SMP in different stages.

As shown in Figure 9b, the average EPS concentrations of two reactors decreased from 97.19 mg·L^{-1} (S1) and 85.92 mg·L^{-1} (S3) to 82.81 mg·L^{-1} (S2) and 81.62 mg·L^{-1} (S4) after the ultrasonic treatment. Biochar addition and ultrasonic treatment were both beneficial to reduce the EPS of sludge in the system, which was beneficial to membrane fouling mitigation. FT-IR spectra were used to characterize the major functional groups of EPS. As shown in Figure 11, the predominant spectral bands were as follows: 2970–2889 cm^{-1} (fatty

acids), 1640 cm^{-1} (Amide I), 1550 cm^{-1} (Amide II), 1400 cm^{-1} (carboxylic groups) and 1047 cm^{-1} (carbohydrates) [61]. The region among 1800–900 cm^{-1} was analyzed in detail because the major bands of amide, carboxylic, and carbohydrate functional groups were included in this zone [62]. The peak at 1640 cm^{-1} was associated with the C=O stretching vibration in secondary protein structures, which existed in all EPS samples and favored bio-flocculation. The band at 1400 cm^{-1} existed in all EPS samples and was caused by the symmetric stretching vibration of deprotonated carboxylic acid groups, which indicated the acidic nature of EPS components [63]. The band at 1040 cm^{-1} were associated with the vibrational stretching of O–H or C–O, the two most common functional groups in any carbohydrate, and the differences in the position and frequency of occurrence of C–O bonds [64]. It can be seen from the position of each peak that the main components in the sludge were protein and polysaccharide, and the reduction of aromatic proteins in EPS could reduce membrane fouling. Therefore, US-AnFMBR was considered to have a significant influence on the concentration reduction and property change of EPS. This may be an important reason for reducing membrane fouling in US-AnFMBR.
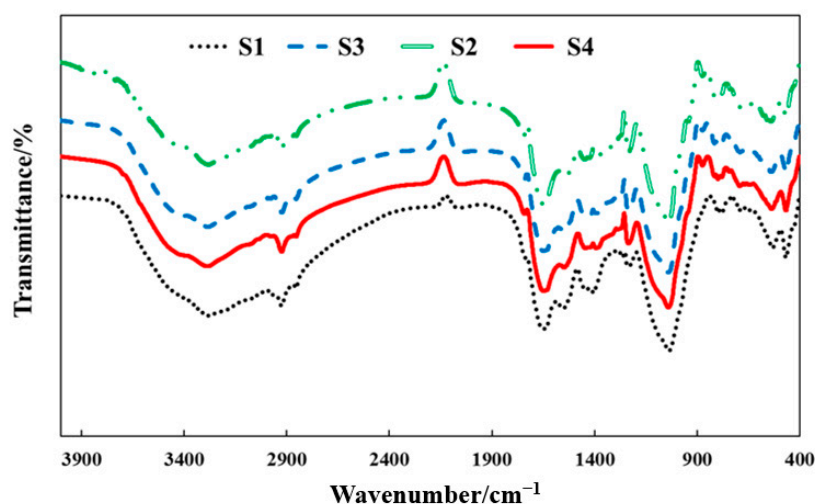

Figure 11. FT-IR spectra of the EPS at different stages.

3.5. Analysis of Agricultural and Environmental Benefits

This study uses AnFMBR in combination with an ultrasonic treatment unit and biochar to create a US-AnFMBR system for the treatment of anaerobically fermented biogas. Usually, the treatment of low C/N sludge digestion liquid requires an additional carbon source, and the input cost is too high. The anaerobic biological treatment process in the US-AnFMBR provides a significant saving in carbon sources. The fluidized pellets in the US-AnFMBR are produced by pyrolysis of pine sawdust and offer new ideas for the use of agricultural waste. The effluent COD concentration after US-AnFMBR (S4) treatment was 119.92 mg·L^{-1}, and the NH$_4^+$-N and PO$_4^{3-}$-P concentrations were 308.41 mg·L^{-1} and 45.25 mg·L^{-1}, respectively. The effluent COD, NH$_4^+$-N and PO$_4^{3-}$-P concentrations all comply with national standards for submersion cultivation and dry farming conditions in China, including the Water Quality Standard for Agricultural Irrigation (GB50842005) and the Water Quality of Agricultural Irrigation Water for Urban Wastewater Recycling (GB209222007). In 2021, the total amount of water used in agriculture in China was 3.64×10^{11} m^3 [65]. The effluent from US-AnFMBR has the potential to provide 1.12×10^7 t NH$_4^+$-N and 1.65×10^6 t PO$_4^{3-}$-P per year to Chinese farmland.

Typical paddy field crops, rice, and dry land crops, wheat, were selected for analysis. The irrigation water requirements for early, middle and late rice are 2700–3450 m^3·ha^{-1}, 3300–3600 m^3·ha^{-1} and 3450–4800 m^3·ha^{-1}, respectively, throughout the growing season, and 150–1200 m^3·ha^{-1} in the case of wheat [66]. Based on the water treatment capacity of the US-AnFMBR, the use of US-AnFMBR effluent as irrigation water pro-

vided 832.71–1480.37 kg·ha^{-1} NH$_4^+$-N and 112.18–17.20 kg·ha^{-1} PO$_4^{3-}$-P for rice and 46.26–370.09 kg·ha^{-1} NH$_4^+$-N for wheat and 6.8–54.30 kg·ha^{-1} PO$_4^{3-}$-P. In China, rice fertilizer use intensities were approximately 48.09 kg·ha^{-1} and 1.13 kg·ha^{-1} for N and P, respectively [63]. The normal fertilizer use intensity for wheat is approximately 56.24 kg·ha^{-1} for N and 1.08 kg·ha^{-1} for P [67]. The US-AnFMBR treated effluent is fully capable of meeting the nutrient requirements of growing crops when used as agricultural irrigation water.

In China, as in many other countries, greenhouse gas emissions from fertilizer production and use are the largest source of total agricultural emissions [68]. Fertilizer application accounts for around 57% of China's total greenhouse gas emissions from agricultural inputs, mainly from the excessive use of nitrogen fertilizers [69]. It is assumed that the source of input N in the farmland is entirely provided by urea (46.8% N content), and the source of P is entirely provided by superphosphate (16.00% P content) [70]. The US-AnFMBR treated effluent was compounded as irrigation water for the rice to reduce the use of 104.55 kg·ha^{-1} of urea and 7.05 kg·ha^{-1} of superphosphate of rice field, respectively. The LCA calculates that the same amount of urea and calcium superphosphate emits a total of 698.57 kg$_{CO2\text{-}eq}$·ha^{-1} of greenhouse gases when used in production and agriculture [70]. In the same way, after the above calculations, the US-AnFMBR effluent was compounded as wheat irrigation water, resulting in a reduction of 122.25 kg·ha^{-1} of urea and 6.75 kg·ha^{-1} of superphosphate used in wheat fields, thus reducing emissions by a total of 699.40 kg$_{CO2\text{-}eq}$·ha^{-1} during fertilizer production and use. The production and use of fertilizers produces approximately 5.5% of China's total greenhouse gas emissions and 9.43–17.1% of global greenhouse gas emissions [69]. In 2021, the area under crop cultivation in China was 1.1763×10^8 ha [71,72]. The use of US-AnFMBR treated effluent as agricultural irrigation water has the potential to reduce greenhouse gas emissions by 8.23×10^7 t$_{CO2\text{-}eq}$ per year. For this reason, the use of US-AnFMBR treated wastewater with a low C/N ratio for agricultural irrigation has good agricultural and environmental benefits.

4. Conclusions

In this study, we report a simple and feasible strategy to establish a US-AnFMBR system by combining an ultrasonic processing unit and biochar in AnFMBR. The system achieves removal of COD, NH$_4^+$-N and PO$_4^{3-}$-P up to 89.41%, 49.29% and 54.83%, showing a better removal effect than normal AnFMBR, and has a better mitigation effect in terms of membrane fouling. Through the analysis of sludge and SMP, it was found that the system can reduce the viscosity of sludge and release more small molecular substances. The low viscosity of sludge can promote the solubilization process of sludge pollutants, and the small molecular substances may pass through the membrane more easily, resulting in a better membrane fouling mitigation. Long-term operation performance also revealed the excellent stability of the sludge digestion liquid treatment. Furthermore, the novel strategy to integrate ultrasonic and biochar with the AnFMBR system in the treatment of sludge digestion liquid can greatly reduce the impact of the sludge digestion liquid returned to the biological treatment unit on the sewage treatment plant, and it can also be used for resource recycling. The effluent from the US-AnFMBR has the potential to provide 1.12×107 t NH$_4^+$-N and 1.65×10^6 t PO$_4^{3-}$-P per year to Chinese farmland, fully meeting the nutrient requirements of growing crops while reducing greenhouse gas emissions by 8.23×107 t$_{CO2\text{-}eq}$ per year. This study is in line with the need for sustainable development of agricultural and environmental practices.

Author Contributions: Conceptualization, L.L.; methodology, Y.C.; data curation, Y.C., Z.G. and G.X.; writing—original draft preparation, L.L.; writing—review and editing, J.Z., Y.T. and S.L.; project

References

1. Cheng, H.; Li, Y.; Guo, G.; Zhang, T.; Qin, Y.; Hao, T.; Li, Y.Y. Advanced methanogenic performance and fouling mechanism investigation of a high-solid anaerobic membrane bioreactor (AnMBR) for the co-digestion of food waste and sewage sludge. *Water Res.* **2020**, *187*, 116436. [CrossRef] [PubMed]
2. Wu, B.; Dai, X.; Chai, X. Critical review on dewatering of sewage sludge: Influential mechanism, conditioning technologies and implications to sludge re-utilizations. *Water Res.* **2020**, *180*, 115912. [CrossRef] [PubMed]
3. Wang, H.; Zhang, J.; Wang, P.; Yin, L.; Tian, Y.; Li, J. Bifunctional copper modified graphitic carbon nitride catalysts for efficient tetracycline removal: Synergy of adsorption and photocatalytic degradation. *Chin. Chem. Lett.* **2020**, *31*, 2789–2794. [CrossRef]
4. Zhen, G.; Lu, X.; Kato, H.; Zhao, Y.; Li, Y.Y. Overview of pretreatment strategies for enhancing sewage sludge disintegration and subsequent anaerobic digestion: Current advances, full-scale application and future perspectives. *Renew. Sustain. Energy Rev.* **2017**, *69*, 559–577. [CrossRef]
5. Zhen, G.; Lu, X.; Li, Y.Y.; Zhao, Y. Combined electrical-alkali pretreatment to increase the anaerobic hydrolysis rate of waste activated sludge during anaerobic digestion. *Appl. Energy* **2014**, *128*, 93–102. [CrossRef]
6. Abelleira-Pereira, J.M.; Perez-Elvira, S.I.; Sanchez-Oneto, J.; de la Cruz, R.; Portela, J.R.; Nebot, E. Enhancement of methane production in mesophilic anaerobic digestion of secondary sewage sludge by advanced thermal hydrolysis pretreatment. *Water Res.* **2015**, *71*, 330–340. [CrossRef]
7. Dereli, R.K.; van der Zee, F.P.; Ozturk, I.; van Lier, J.B. Treatment of cheese whey by a cross-flow anaerobic membrane bioreactor: Biological and filtration performance. *Environ. Res.* **2019**, *168*, 109–117. [CrossRef]
8. van Loosdrecht, M.C.; Salem, S. Biological treatment of sludge digester liquids. *Water Sci. Technol.* **2006**, *53*, 11–20. [CrossRef]
9. Janus, H.F.v.d.R.H.M. Don't reject the idea of treating reject water. *Water Sci. Technol.* **1997**, *35*, 27–34. [CrossRef]
10. Song, X.; Luo, W.; Nguyen, L.N.; Ngo, H.H.; Guo, W.; Nghiem, L.D. Anaerobic membrane bioreactors for emerging pollutants removal. *Current Developments in Biotechnology and Bioengineering*. 2020, pp. 197–218. Available online: https://www.researchgate.net/publication/339098808_Anaerobic_membrane_bioreactors_for_emerging_pollutants_removal (accessed on 4 November 2022).
11. Wang, J.L.; Wang, S.Y.; Gao, Y.Q. Nitrogen Removal by Simultaneous Nitrification and Denitrification via Nitrite in a Sequence Hybrid Biological Reactor. *Chin. J. Chem. Eng.* **2008**, *16*, 778–784. [CrossRef]
12. Claros, J.; Serralta, J.; Seco, A.; Ferrer, J.; Aguado, D. Real-time control strategy for nitrogen removal via nitrite in a SHARON reactor using pH and ORP sensors. *Process Biochem.* **2012**, *47*, 1510–1515. [CrossRef]
13. Fux, C.; Boehler, M.; Philipp, H.; Irene, B.; Hansruedi, S. Biological treatment of ammonium-rich wastewater by partial nitration and subsequent anaerobic ammonium oxidation (anammox) in a pilot plant. *J. Biotechnol.* **2002**, *99*, 295–306. [CrossRef] [PubMed]
14. Dapena-Mora, A.; Van Hulle, S.W.H.; Luis Campos, J.; Méndez, R.; Vanrolleghem, P.A.; Jetten, M. Enrichment of Anammox biomass from municipal activated sludge: Experimental and modelling results. *J. Chem. Technol. Biotechnol.* **2004**, *79*, 1421–1428. [CrossRef]
15. Kolisch, G.; Rolfs, T. Integrated sidestream treatment for enhanced enlargement of sewage plants. *Water Sci. Technol.* **2000**, *41*, 155–162. [CrossRef]
16. Volcke, E.I.; Loccufier, M.; Noldus, E.J.; Vanrolleghem, P.A. Operation of a SHARON nitritation reactor: Practical implications from a theoretical study. *Water Sci. Technol.* **2007**, *56*, 145–154. [CrossRef]
17. Vandevivere, P. New and Broader Applications of Anaerobic Digestion. *Crit. Rev. Environ. Sci. Technol.* **1999**, *29*, 151–173. [CrossRef]
18. Kong, Z.; Wu, J.; Rong, C.; Wang, T.; Li, L.; Luo, Z.; Ji, J.; Hanaoka, T.; Sakemi, S.; Ito, M.; et al. Sludge yield and degradation of suspended solids by a large pilot-scale anaerobic membrane bioreactor for the treatment of real municipal wastewater at 25 °C. *Sci. Total Environ.* **2021**, *759*, 143526. [CrossRef]

19. McCarty, P.L.; Bae, J.; Kim, J. Domestic Wastewater Treatment as a Net Energy Producer–Can This be Achieved? *Environ. Sci. Technol.* **2011**, *45*, 7100–7106. [CrossRef]

20. Seib, M.D.; Berg, K.J.; Zitomer, D.H. Low energy anaerobic membrane bioreactor for municipal wastewater treatment. *J. Membr. Sci.* **2016**, *514*, 450–457. [CrossRef]

21. Gao, D.W.; Hu, Q.; Yao, C.; Ren, N.Q.; Wu, W.M. Integrated anaerobic fluidized-bed membrane bioreactor for domestic wastewater treatment. *Chem. Eng. J.* **2014**, *240*, 362–368. [CrossRef]

22. Xiao, X.; Huang, Z.; Ruan, W.; Yan, L.; Miao, H.; Ren, H.; Zhao, M. Evaluation and characterization during the anaerobic digestion of high-strength kitchen waste slurry via a pilot-scale anaerobic membrane bioreactor. *Bioresour. Technol.* **2015**, *193*, 234–242. [CrossRef]

23. Ying, Z.; Ping, G. Effect of powdered activated carbon dosage on retarding membrane fouling in MBR. *Sep. Purif. Technol.* **2006**, *52*, 154–160. [CrossRef]

24. Chaiprapat, S.; Thongsai, A.; Charnnok, B.; Khongnakorn, W.; Bae, J. Influences of liquid, solid, and gas media circulation in anaerobic membrane bioreactor (AnMBR) as a post treatment alternative of aerobic system in seafood industry. *J. Membr. Sci.* **2016**, *509*, 116–124. [CrossRef]

25. Liu, L.; Wang, X.; Fang, W.; Li, X.; Shan, D.; Dai, Y. Adsorption of metolachlor by a novel magnetic illite-biochar and recovery from soil. *Environ. Res.* **2022**, *204*, 111919. [CrossRef]

26. Liu, L.; Li, X.; Wang, X.; Wang, Y.; Shao, Z.; Liu, X.; Shan, D.; Liu, Z.; Dai, Y. Metolachlor adsorption using walnut shell biochar modified by soil minerals. *Environ. Pollut.* **2022**, *308*, 119610. [CrossRef]

27. Sohn, W.; Guo, W.; Ngo, H.; Deng, L.; Cheng, D.; Zhang, X. A review on membrane fouling control in anaerobic membrane bioreactors by adding performance enhancers. *J. Water Process Eng.* **2021**, *40*, 101867. [CrossRef]

28. Li, Y.; Xu, D.; Lin, H.; Wang, W.; Yang, H. Nutrient released characteristics of struvite-biochar fertilizer produced from concentrated sludge supernatant by fluidized bed reactor. *J. Environ. Manag.* **2023**, *325*, 116548. [CrossRef]

29. Ruiz-Hernando, M.; Martinez-Elorza, G.; Labanda, J.; Llorens, J. Dewaterability of sewage sludge by ultrasonic, thermal and chemical treatments. *Chem. Eng. J.* **2013**, *230*, 102–110. [CrossRef]

30. Zhang, G.; Zhang, P.; Gao, J.; Chen, Y. Using acoustic cavitation to improve the bio-activity of activated sludge. *Bioresour. Technol.* **2008**, *99*, 1497–1502. [CrossRef]

31. Lippert, T. Sewage Sludge Disintegration Using Innovative Ultrasound Reactors with Surface Transducers-Performance Assessment and Optimization of Operating Conditions. Ph.D. Thesis, Technical University of Munich, Munich, Germany, 2021.

32. Nour, A.H.; Zaki, Y.H.; Mohamed, H.S.; Rassem, H.H. The Potentials of an Integrated Ultrasonic Membrane Anaerobic System (IUMAS) in Treating Sugar Cane Wastewater. *Indones. J. Chem.* **2019**, *19*, 804–810. [CrossRef]

33. Tyagi, V.K.; Lo, S.L.; Appels, L.; Dewil, R. Ultrasonic treatment of waste sludge: A review on mechanisms and applications. *Crit. Rev. Env. Sci. Tec.* **2014**, *44*, 1220–1288. [CrossRef]

34. Chowdhury, M.M.I.; Nakhla, G.; Zhu, J. Ultrasonically enhanced anaerobic digestion of thickened waste activated sludge using fluidized bed reactors. *Appl. Energy* **2017**, *204*, 807–818. [CrossRef]

35. Zhang, X.; Liu, Y.; Li, Z.R.; Zhang, J.; Chen, Y.; Wang, Q. Impact of COD/N on anammox granular sludge with different biological carriers. *Sci. Total Environ.* **2020**, *28*, 138557. [CrossRef] [PubMed]

36. Luna, H.J.; Baêta, B.E.L.; Aquino, S.F.; Susa, M.S.R. EPS and SMP dynamics at different heights of a submerged anaerobic membrane bioreactor (SAMBR). *Process Biochem.* **2014**, *49*, 2241–2248. [CrossRef]

37. Meng, F.; Chae, S.R.; Drews, A.; Kraume, M.; Shin, H.S.; Yang, F. Recent advances in membrane bioreactors (MBRs): Membrane fouling and membrane material. *Water Res.* **2009**, *43*, 1489–1512. [CrossRef]

38. Laspidou, C.S.; Rittmann, B. A unified theory for extracellular polymeric substances, soluble microbial products, and active and inert biomass. *Water Res.* **2002**, *36*, 2711–2720. [CrossRef] [PubMed]

39. Choo, K.H.; Lee, C.H. Hydrodynamic behavior of anaerobic biosolids during crossflow filtration in the membrane anaerobic bioreactor. *Water Res.* **1998**, *32*, 3387–3397. [CrossRef]

40. Hahilton, J.K. Colorimetric Method for Determination of Sugars and Related Substances. *Anal. Chem.* **1956**, *28*, 350–356.

41. Frølund, T.G.B.; Nielsen, P.H. Enzymatic activity in the activated-sludge floc matrix. *Appl. Microbiol. Biotechnol.* **1995**, *43*, 755–761. [CrossRef]

42. Clurman, A.M.; Rodríguez-Narvaez, O.M.; Jayarathne, A.; De Silva, G.; Ranasinghe, M.I.; Goonetilleke, A.; Bandala, E.R. Influence of surface hydrophobicity/hydrophilicity of biochar on the removal of emerging contaminants. *Chem. Eng. J.* **2020**, *402*, 126277. [CrossRef]

43. Quarmby, J.; Scott, J.R.; Mason, A.K.; Davies, G.; Parsons, S.A. The application of ultrasound as a pre-treatment for anaerobic digestion. *Environ. Technol.* **2010**, *20*, 1155–1161. [CrossRef]

44. Wang, J.; Wu, B.; Chew, J.W. Membrane fouling mitigation by fluidized granular activated carbon: Effect of fiber looseness and impact on irreversible fouling. *Sep. Purif. Technol.* **2020**, *242*, 116764. [CrossRef]

45. Sima, X.F.; Wang, Y.Y.; Shen, X.C.; Jing, X.R.; Tian, L.J.; Yu, H.Q.; Jiang, H. Robust biochar-assisted alleviation of membrane fouling in MBRs by indirect mechanism. *Sep. Purif. Technnol.* **2017**, *184*, 195–204. [CrossRef]

46. Kim, M.; Lam, T.Y.C.; Tan, G.-Y.A.; Lee, P.H.; Kim, J. Use of polymeric scouring agent as fluidized media in anaerobic fluidized bed membrane bioreactor for wastewater treatment: System performance and microbial community. *J. Membr. Sci.* **2020**, *606*, 118121. [CrossRef]

47. Fortunato, L.; Pathak, N.; Ur Rehman, Z.; Shon, H.; Leiknes, T. Real-time monitoring of membrane fouling development during early stages of activated sludge membrane bioreactor operation. *Process Saf. Environ.* **2018**, *120*, 313–320. [CrossRef]

48. Wang, J.; Wu, B.; Liu, Y.; Fane, A.G.; Chew, J.W. Monitoring local membrane fouling mitigation by fluidized GAC in lab-scale and pilot-scale AnFMBRs. *Sep. Purif. Technol.* **2018**, *199*, 331–345. [CrossRef]

49. Berkessa, Y.W.; Yan, B.; Li, T.; Jegatheesan, V.; Zhang, Y. Treatment of anthraquinone dye textile wastewater using anaerobic dynamic membrane bioreactor: Performance and microbial dynamics. *Chemosphere* **2020**, *238*, 124539. [CrossRef]

50. Yu, W.; Graham, N.; Liu, T. Effect of intermittent ultrasound on controlling membrane fouling with coagulation pre-treatment: Significance of the nature of adsorbed organic matter. *J. Membr. Sci.* **2017**, *535*, 168–177. [CrossRef]

51. Aghapour Aktij, S.; Taghipour, A.; Rahimpour, A.; Mollahosseini, A.; Tiraferri, A. A critical review on ultrasonic-assisted fouling control and cleaning of fouled membranes. *Ultrasonics* **2020**, *108*, 106228. [CrossRef] [PubMed]

52. Lin, Y.H.; Tung, K.L.; Wang, S.H.; Zhou, Q.; Shung, K.K. Distribution and deposition of organic fouling on the microfiltration membrane evaluated by high-frequency ultrasound. *J. Membr. Sci.* **2013**, *433*, 100–111. [CrossRef]

53. Pilli, S.; Bhunia, P.; Yan, S.; LeBlanc, R.J.; Tyagi, R.D.; Surampalli, R.Y. Ultrasonic pretreatment of sludge: A review. *Ultrason. Sonochem.* **2011**, *18*, 1–18. [CrossRef] [PubMed]

54. Xu, M.; Wen, X.; Huang, X.; Yu, Z.; Zhu, M. Mechanisms of membrane fouling controlled by online ultrasound in an anaerobic membrane bioreactor for digestion of waste activated sludge. *J. Membr. Sci.* **2013**, *445*, 119–126. [CrossRef]

55. Le, N.T.; Julcour-Lebigue, C.; Delmas, H. Ultrasonic sludge pretreatment under pressure. *Ultrason. Sonochem.* **2013**, *20*, 1203–1210. [CrossRef]

56. Xiang, W.; Zhang, X.; Chen, J.; Zou, W.; He, F.; Hu, X.; Tsang, D.C.W.; Ok, Y.S.; Gao, B. Biochar technology in wastewater treatment: A critical review. *Chemosphere* **2020**, *252*, 126539. [CrossRef]

57. Ming, J.; Wang, Q.; Yoza, B.A.; Liang, J.; Guo, H.; Li, J.; Guo, S.; Chen, C. Bioreactor performance using biochar and its effect on aerobic granulation. *Bioresour. Technol.* **2020**, *300*, 122620. [CrossRef] [PubMed]

58. Joshi, P.; Parker, W. Effect of pretreatment using ultrasound and hydrogen peroxide on digestion of waste activated sludge in an anaerobic membrane bioreactor. *Environ. Prog. Sustain.* **2015**, *34*, 1724–1730. [CrossRef]

59. Teng, J.; Shen, L.; Xu, Y.; Chen, Y.; Wu, X.L.; He, Y.; Chen, J.; Lin, H. Effects of molecular weight distribution of soluble microbial products (SMPs) on membrane fouling in a membrane bioreactor (MBR): Novel mechanistic insights. *Chemosphere* **2020**, *248*, 126013. [CrossRef]

60. Chen, L.; Cheng, P.; Ye, L.; Chen, H.; Xu, X.; Zhu, L. Biological performance and fouling mitigation in the biochar-amended anaerobic membrane bioreactor (AnMBR) treating pharmaceutical wastewater. *Bioresour. Technol.* **2020**, *302*, 122805. [CrossRef]

61. Zhu, L.; Qi, H.Y.; Lv, M.L.; Kong, Y.; Yu, Y.W.; Xu, X.Y. Component analysis of extracellular polymeric substances (EPS) during aerobic sludge granulation using FTIR and 3D-EEM technologies. *Bioresour. Technol.* **2012**, *124*, 455–459. [CrossRef]

62. Jurgen Schmitt, H.C.F. c-spectroscopy in microbial and material analysis. *Int. Biodeterior. Biodegrad.* **1998**, *41*, 1–11. [CrossRef]

63. Badireddy, A.R.; Chellam, S.; Gassman, P.L.; Engelhard, M.H.; Lea, A.S.; Rosso, K.M. Role of extracellular polymeric substances in bioflocculation of activated sludge microorganisms under glucose-controlled conditions. *Water Res.* **2010**, *44*, 4505–4516. [CrossRef]

64. Mecozzi, M.; Pietrantonio, E. Carbohydrates proteins and lipids in fulvic and humic acids of sediments and its relationships with mucilaginous aggregates in the Italian seas. *Mar. Chem.* **2006**, *101*, 27–39. [CrossRef]

65. China Water Resources Bulletin. 2021. Available online: https://www.ndrc.gov.cn/fggz/dqjj/qt/202207/t20220701_1329874_ext.html (accessed on 4 November 2022).

66. Chen, Y.; Guo, G.; Wang, G.; Kang, S.; Luo, H.; Zhang, D. *Main Crop Water Requirement and Irrigation of China*; Water Resources & Hydropower Press: Beijing, China, 1995.

67. Price Department of the National Development and Reform Commission (PDNDRC). *National Agricultural Products Cost-Benefit Compilation*; China Statistics Press: Beijing, China, 2017.

68. Liu, Y.L.; Zhou, Z.Q.; Zhang, X.X.; Xu, X.; Chen, H.; Xiong, Z.Q. Net global warming potential and greenhouse gas intensity from the double rice system with integrated soil-crop system management: A three-year field study. *Atmos. Environ.* **2015**, *116*, 92–101. [CrossRef]

69. Wu, H.J.; MacDonald, G.K.; Galloway, J.N.; Zhang, L.; Gao, L.M.; Yang, L.; Yang, J.X.; Li, X.L.; Li, H.R.; Yang, T. The influence of crop and chemical fertilizer combinations on greenhouse gas emissions: A partial life-cycle assessment of fertilizer production and use in China. *Resour. Conserv. Recycl.* **2021**, *168*, 105303. [CrossRef]

70. Chen, S.; Lu, F.; Wang, X.K. Estimation of greenhouse gases emission factors for China's nitrogen, phosphate, and potash fertilizers. *Acta Ecol. Sin.* **2015**, *35*, 6371–6383.

71. Liu, L.; Liu, Z.; Wang, S.; Liu, Y.; Sun, M.; Dai, Y. Can biochar fulfill the nitrogen need of maize under reduced nitrogen input? *Environ. Eng. Manag. J.* **2023**, *21*, 1815–1824.

72. National Economic and Social Development Statistical Bulletin. 2021. Available online: http://www.stats.gov.cn/ (accessed on 4 November 2022).